

Size segregated aerosol mass concentration measurements over the Arabian Sea during ICARB

VIJAYAKUMAR S NAIR¹, K KRISHNA MOORTHY¹, S SURESH BABU¹, K NARASIMHULU²,
L SIVA SANKARA REDDY², R RAMAKRISHNA REDDY², K RAMA GOPAL²,
V SREEKANTH³, B L MADHAVAN³ and K NIRANJAN³

¹*Space Physics Laboratory, Vikram Sarabhai Space Centre, Trivandrum 695 022, India.*

²*Department of Physics, Sri Krishnadevaraya University, Anantapur 515 003, India.*

³*Department of Physics, Andhra University, Visakhapatnam 530 003, India.*

Mass concentration and mass size distribution of total (composite) aerosols near the surface are essential inputs needed in developing aerosol models for radiative forcing estimation as well as to infer the environment and air quality. Using extensive measurements onboard the oceanographic research vessel, *Sagar Kanya*, during its cruise SK223B in the second phase of the ocean segment of the Integrated Campaign for Aerosols, gases and Radiation Budget (ICARB), the spatial distribution of the mass concentration and mass size distribution of near-surface aerosols are examined for the first time over the entire Arabian Sea, going as far as 58°E and 22°N, within a span of 26 days. In general, the mass concentrations (M_T) were found to be low with the mean value for the entire Arabian Sea being $16.7 \pm 7 \mu\text{g m}^{-3}$; almost 1/2 of the values reported in some of the earlier campaigns. Coarse mode aerosols contributed, on an average, 58% to the total mass, even though at a few pockets accumulation mode contribution dominated. Spatially, significant variations were observed over central and northern Arabian Sea as well as close to the west coast of India. In central Arabian Sea, even though the M_T was quite low, contribution of accumulation aerosols to the total mass concentration was greater than 50%. Effective radius, a parameter important in determining scattering properties of aerosol size distribution, varied between 0.07 and $0.4 \mu\text{m}$ with a mean value of $0.2 \mu\text{m}$. Number size distributions, deduced from the mass size distributions, were approximated to inverse power-law form and the size indices (ν) were estimated. It was found to vary in the range 3.9 to 4.2 with a mean value of 4.0 for the entire oceanic region. Extinction coefficients, estimated using the number-size distributions, were well-correlated with the accumulation mode mass concentration with a correlation coefficient of 0.82.

1. Introduction

Characterization of aerosol properties is crucial in radiation balance assessment of the earth-atmosphere system due to (i) the interaction of aerosols with solar and terrestrial radiation through scattering and absorption and (ii) the modification of cloud properties, lifetime and albedo (Twomey 1977; Charlson *et al* 1992; IPCC 2007). Extensive field campaigns during the last

decade over the different oceanic regions of the world have brought out significant spatial and temporal heterogeneities of physical, chemical, and optical properties of atmospheric aerosols, particularly over oceans surrounded by large landmasses (e.g., Prospero 1979; Smirnov *et al* 1995; Sakerin and Kabanov 2002; Moorthy *et al* 2005a). In the Indian context, the investigation of aerosol characteristics over oceans surrounding India were limited to the Indian Ocean Experiment (INDOEX,

Keywords. Aerosol mass concentration; Arabian Sea; ICARB.

Ramanathan *et al* 2001) focusing on the northern Indian Ocean during winter season; the Arabian Sea Monsoon Experiment (ARMEX, Moorthy *et al* 2005a), which addressed the small warm pool region in the southeast Arabian Sea during inter monsoon and summer monsoon seasons; and a few short cruises along the Indian coastal waters (Satheesh and Moorthy 1997; Vinoj and Satheesh 2003). Besides, some measurements are available, again for the winter season, based on an extensive road campaign along the west coast of peninsular India (Moorthy *et al* 2005b). Extensive investigation covering coastal as well as central regions of Arabian Sea or Bay of Bengal have not been attempted earlier, which is essential to understand the spatial heterogeneity over oceans, the impact of different land regions like east Asia, west Asia and Africa in modifying the aerosol properties by interacting with the prevailing, regional and mesoscale meteorology. In this context, mass concentration and mass size distribution of total aerosols near the surface are essential inputs needed in developing aerosol models for radiative forcing estimation as well as to infer environment and air quality. ICARB (Moorthy *et al* 2006) was designed to address this aspect. During the campaign, continuous and simultaneous measurements of aerosols were carried out from ship, aircraft and fixed land stations to infer their properties over the Indian subcontinent and oceanic regions surrounding it. In this paper we present the spatial variation of mass concentration and size distribution of composite (total) aerosols in the marine atmospheric boundary layer over the vast areas of the Arabian Sea.

2. Cruise details, data, and analysis

During the second leg of the ocean segment of ICARB, extensive measurements of aerosols were made onboard the cruise SK223B of the Oceanographic Research Vessel (ORV) *Sagar Kanya* (SK) over the Arabian Sea (AS) covering regions from west coastal India to as far as close to the east coast of Somalia and Oman, bounded between latitudes 9°N to 21°N, within a span of 26 days. The cruise commenced from the port of Kochi (10.0°N, 76.2°E) on 18 April 2006 and the expedition terminated at Goa (15.4°N, 73.7°E) on 11 May 2006. The cruise track is shown in figure 1 by the solid line, while the daily position of the ship at 05:30 UTC is depicted by the circles with the dates below them. The major ports on the west coast of India and Arabia are also shown in the figure. Aerosol measurements onboard the ORV were carried out from a specially designed laboratory on the top deck (B deck) using iso-kinetic, community air inlet which ensured the same ambient

conditions for all the measurements (Moorthy *et al* 2006).

Size-segregated measurements of aerosol mass concentrations were carried out using a 10-stage quartz crystal microbalance (QCM) cascade impactor (model PC2 of California measurements inc., USA), having lower cut-off (50%) at particle diameters >25, 12.5, 6.4, 3.2, 1.6, 0.8, 0.4, 0.2, 0.1, and 0.05 μm respectively for stages 1 to 10. The flow rate was maintained 0.24 litre min^{-1} and typical sampling interval was 300 seconds. The particle diameters (dp) provided by the QCM are derived from its intrinsic aerodynamic diameter (da) assuming a particle density (ρ) of 2 g cm^{-3} and the relation $dp = da/\sqrt{\rho}$. As such, any deviation in the actual density from 2 g cm^{-3} will result in a corresponding shift in the stage cut-off diameters (Pillai and Moorthy 2001), though however, the total mass concentrations are not affected. Inertially separated aerosol particles deposit on a piezo-electric sensing crystal (in each stage) and the change in the beat frequency with respect to the reference crystal oscillator of the same stage is calibrated in terms of the particle mass. Effect of variations in ambient temperature and humidity were nullified by using matched crystal pairs in each stage. More details are available in Pillai and Moorthy (2001). Continuous measurements required frequent cleaning of the sensing crystal and this was done as per the instrument protocol. On average, 30 measurements were available for each day at an average interval of 45 min as observations were made round the clock. Measurements were limited to relative humidity (deck level) < 75%, in view of the sensitivity of the QCM to RH changes at high RH. Details of data analysis and error budgeting are available in Pillai and Moorthy (2001). Comparison of QCM measured mass concentrations have shown in general, a good agreement with those measured by other means, such as using high volume samplers, under a variety of environmental conditions (Moorthy *et al* 2005b).

3. Synoptic meteorology

The mean synoptic wind pattern (derived from the NCEP-NCAR reanalysis data) that prevailed at 850 hPa over the AS during the campaign period (figure 2) comprised of strong (>5 m s^{-1}) westerlies over the northern AS (north of 16°N) and weaker (<3 m s^{-1}) northerly or northeasterly over the southern AS (south of 15°N). A low level anticyclone centered at 16°N, 63°E caused the northwesterly winds to turn down southward, and resulted in winds that were stronger as we moved closer to the Indian coast. A region of very low wind prevailed in central AS associated

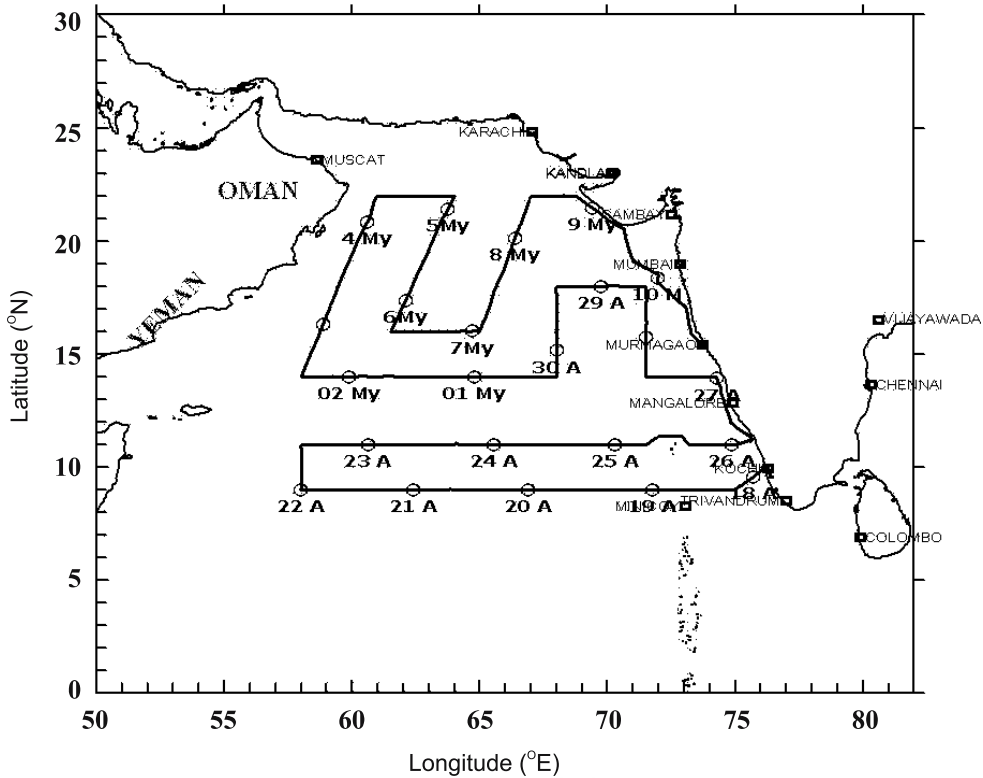


Figure 1. The cruise track of SK223B. The continuous lines show the cruise track with the daily position of the ship at 05:30 UTC, being denoted by the circles on the track line.

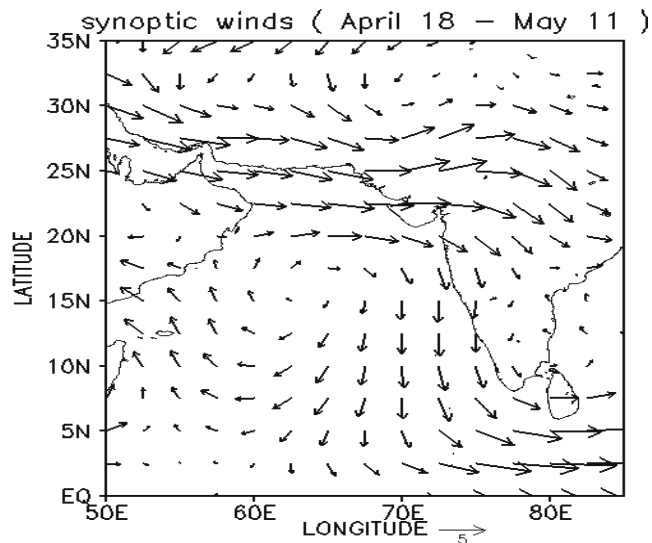


Figure 2. Mean synoptic wind vectors at 850 hPa for April–May 2006.

with the anticyclone. Relative humidity varied from 55% to 90% with an average value of 70%. Precipitation was absent throughout the cruise period. The whole campaign period was characterized by fair weather and the absence of any major weather events, cyclones, or depressions over the Arabian Sea.

4. Results and discussion

Total aerosol mass concentration ($M_T = \sum m_i$, where m_i is the mass concentration on the individual stages) varied from the lowest value of $5 \mu\text{g m}^{-3}$ to the highest value of $45 \mu\text{g m}^{-3}$ over the Arabian Sea, with a mean value of $16.7 \pm 7 \mu\text{g m}^{-3}$ during the cruise period. The spatial distribution of M_T is shown in figure 3. Here it should be emphasized that such a representation implicitly assumes temporal stability (statistical) of the aerosol properties during the campaign period. To realize such conditions as close as possible, the cruise was carried out during a meteorologically calm period. Moreover, we had three observation sites; two along the west coast of peninsular India (Trivandrum and Pune) and one island station (Minicoy) in the southeastern Arabian Sea, to examine temporal variations during the campaign. The results, particularly from Minicoy (which appears in a companion paper) indicated that temporal variations were small during the campaign period. The above holds good for other spatial features discussed in the succeeding sections (where we deal with figures 4 and 5). In general, the mass concentrations over the AS were remarkably lower than those reported during the INDOEX cruises (Parameswaran *et al* 1999; Ramachandran and Jayaraman 2002) even

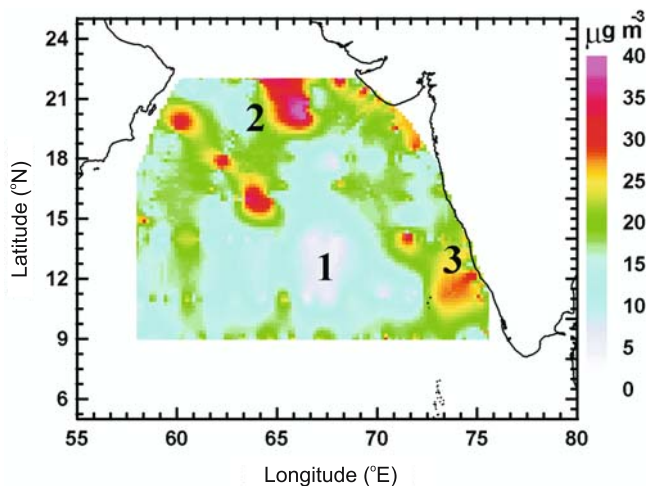


Figure 3. Spatial variation of total mass concentration over the Arabian Sea. Regions deviated from the mean pattern were marked as 1, 2 and 3.

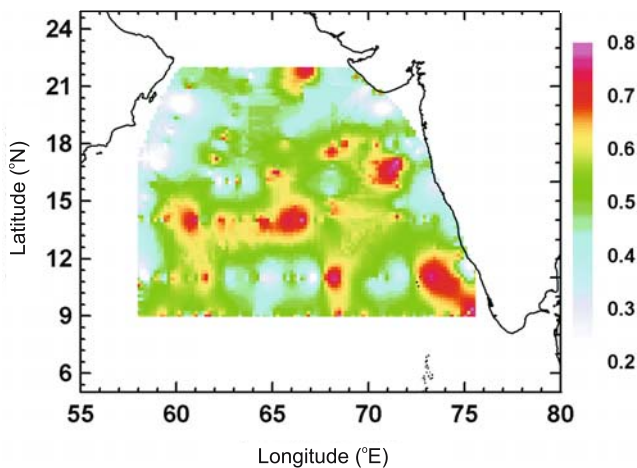


Figure 4. Spatial variation of the fraction of accumulation mode aerosols to the total mass concentration over the entire Arabian Sea.

though those measurements were carried out at near and far coastal regions of the AS during February 1998 and mid AS during April 1999. Interestingly, during ICARB, about 60% of the M_T values were between 10 to $18 \mu\text{g m}^{-3}$. Significant deviations from the mean pattern were observed mainly in three regions (1) central AS ($10\text{--}15^\circ\text{N}$ and $65\text{--}70^\circ\text{E}$), (2) northern AS ($19\text{--}22^\circ\text{N}$ and $64\text{--}68^\circ\text{E}$) and (3) along the west coast of peninsular India. These regions are marked as 1, 2, and 3 in figure 3 and are examined in detail.

Region (1). Extremely low mass loading was observed over the south and central AS; the region bounded between 10 to 15°N in latitude and 65 to 70°E in longitude where the anticyclone prevailed. Total mass concentration over this region was always $< 15 \mu\text{g m}^{-3}$ (mean $8.2 \pm 4.1 \mu\text{g m}^{-3}$).

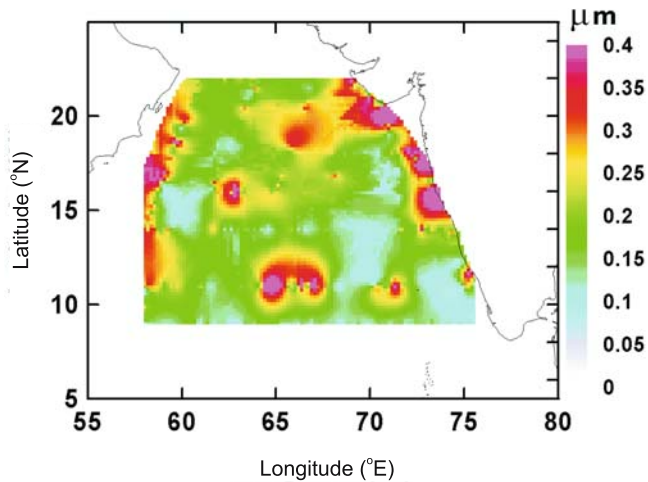


Figure 5. Spatial variation of effective radius over the Arabian Sea.

These low values of M_T appear to be associated with the anticyclonic (subsidence) wind pattern that persisted over this region (figure 2). Normally a subsidence is expected to cause an increase in the near-surface aerosol concentration due to vertical confinement and accumulation of particles. However, in the absence of aerosols (by transport) at higher levels (so that the particle abundance is very low at the higher levels) and no advection at lower levels, the net aerosol concentrations will be decided by the rate of local production (bubble bursting) and scavenging mechanisms (dry and wet deposition) (e.g., Zhang *et al* 2001; Hoppel *et al* 2002). During our campaign, sea surface wind speed in this region was comparable to those outside this region of AS, so that the local production of sea salt through bubble bursting is not significantly different. However, the vertical winds, derived from NCEP, show strong descent (values going as high as 0.08 hPa s^{-1}) at 850 hPa over this region during the period of measurements. These are very high values for vertical velocities. The five-day air mass back trajectories (at 500 m amsl) estimated using HYSPLIT (Hybrid Single Particle Lagrangian Integrated Trajectory) model for all the days of measurements in region 1, were confined within the AS indicating absence of any significant long-range transport from the adjoining continents. Under these conditions, following Hoppel *et al* (2002), the concentrations of particles with radius below $5 \mu\text{m}$ in marine atmospheric boundary layer (MABL) are determined by the entrainment (or vertical) wind velocity than the fall velocity. This strong downdraft (vertical wind) accelerated the particle loss by dry deposition on the sea surface and resulted in the depletion of M_T . This is more efficient at larger sizes, which contribute significantly to the mass loading. During

the Second Aerosol Characterisation Experiment (ACE-2) over the sub-tropical north-east Atlantic Ocean, Hoell *et al* (2000) have shown significant reduction in aerosol number concentration in association with the entrainment of sub-micron free troposphere (FT) aerosols into the marine boundary layer (MABL), thus altering the aerosol properties.

Region (2). Northern AS (19–22°N and 64–68°E) showed very high values of M_T (mean $20.6 \pm 9 \mu\text{g m}^{-3}$). Such a region of enhanced aerosol concentration and optical depth in the northern central AS (around the same region as region 2) has been reported earlier (Parameswaran *et al* 1999; Moorthy and Saha 2000; Kamra *et al* 2001; Moorthy *et al* 2001). Moorthy and Saha (2000), based on AOD measurements during INDOEX cruises of 1998 and 1999, found a pocket of high AOD in the northern central Arabian Sea (around region 2), which they called the ‘west Asian High’ due to its proximity to west Asia and attributed this high in aerosol loading to the transport from the west Asia (Prospero 1979; Moorthy and Saha 2000). Via model applications, Tegen *et al* (1996) have also shown that northern AS is the most mineral dust affected oceanic region. Impacts of west Asian mineral dust transport on aerosol properties over the AS and its influence on aerosol direct short wave radiative forcing have also been reported during this period (Satheesh and Srinivasan 2002; Moorthy *et al* 2005a). Five-day air mass back trajectory analysis using HYSPLIT model at 500 m amsl for the measurement days in which the ship was in this region showed advection patterns along the Oman coast. Thus, advection of aerosols from these arid regions is a strong candidate for the observed high mass concentration over northern AS.

Region (3). Moderate mass concentrations with a mean value of $16.3 \pm 7 \mu\text{g m}^{-3}$, persisted along the west coast of India with higher values very near to the ports. Anthropogenic activities in the industrialized, urban areas and ports along the west coast of peninsular India (such as Kochi, Mangalore, Goa and Mumbai) and several other smaller ports and fishing harbours in between strongly influence M_T over the coastal regions. The advection of these continental aerosols, which are smaller in size, over the marine environment increases the optical depth as well as mass loading (Moorthy *et al* 2005a). During the INDOEX campaign, extremely high values of aerosol mass concentrations were reported over the coastal and northern Indian Ocean and these were attributed to the advection of anthropogenic aerosols produced from the mainland (Novakov *et al* 2000; Ramanathan *et al* 2001). Even though

our measurements show higher mass concentration near to the west coast of peninsular India, the absolute values are much lower than those reported during the INDOEX.

Now we compare our results obtained during the ICARB for the whole AS, with other results reported from this region by other less extensive measurements. Mean M_T over AS in our study is $16.7 \pm 7 \mu\text{g m}^{-3}$ and it is comparable to the values reported over rather pristine oceanic regions of southern hemisphere (Moorthy *et al* 2005c; Ball *et al* 2003). A comparison of our results with those obtained from earlier measurements of M_T over different regions of the Arabian Sea is given in table 1 along with the references. It is interesting to note that the mean M_T values over the different regions of AS during ICARB are less than half of the values reported during the earlier measurements.

4.1 Accumulation and coarse mode fractions

Accumulation mode aerosols (with radii $< 1.0 \mu\text{m}$) are most effective in interacting with the UV and the visible part of the solar spectrum. As the fine mode aerosol concentration increases, the spectral dependence of aerosol optical depths becomes steeper. The dominance of accumulation mode aerosols is generally attributed to anthropogenic influence from the mainland/continent. However, a few studies have shown that significant contribution to accumulation particle can also come from the wind-borne submicron sea salt aerosols with sizes going even below $0.3 \mu\text{m}$ (O’Dowd and Smith 1993; O’Dowd *et al* 1997). From the size resolved measurements of the mass concentration using QCM, we estimated the mass concentration (M_A) of accumulation mode aerosols (with radii $< 1 \mu\text{m}$; stages 7 to 10 of QCM) and M_C of coarse mode aerosols (with radii $> 1 \mu\text{m}$, stages 1 to 6 of QCM). Figure 4 shows the spatial distribution of accumulation mode fraction ($A_F = M_A/M_T$) over the AS. Enhanced dominance of accumulation mode aerosols (with $A_F > 0.7$) is seen only along the southwest coast of India, especially near the highly industrialized ports indicating the advection of continental aerosols from the peninsula. It is also very interesting to note the higher percentage contribution of accumulation fraction at the northern AS, which may be attributed to the anthropogenic aerosols advected along with fine mineral dust from the west Asian regions to AS. Transported mineral dust is known to be mostly in accumulation size ranges with a typical mode radius of $0.5 \mu\text{m}$ (Hess *et al* 1998), since larger particles are removed faster from the atmosphere (by sedimentation) close to the source regions. It may also be recalled at this juncture that based on a road campaign in 2004, Moorthy *et al* (2005b) have

Table 1. Comparison of the average total mass concentrations in different regions of the Arabian Sea as seen during the ICARB with those reported from earlier measurements.

Region 1	Region 2	Region 3	Whole Arabian Sea	Campaign	References
–	–	29.7 ± 1.1	–	ARMEX-II (March–April 2003)	Moorthy <i>et al</i> (2005a)
41.3 ± 6	–	48.0 ± 4	–	INDOEX – FFP (1998) (February 1998)	Parameswaran <i>et al</i> (1999)
25.8	–	–	–	INDOEX – IFP (1999) (March 1999)	Quinn <i>et al</i> (2002) Ball <i>et al</i> (2003)
–	~50 (Average for the entire data)	–	–	INDOEX and 4 short cruises (Average for 4 years, January to April)	Ramachandran and Jayaraman (2002)
–	–	35.6 ± 12	–	INDOEX 98 and 99 (February–March 1998, 1999)	Nair <i>et al</i> (2005)
8.2 ± 4.1	20.6 ± 9	16.4 ± 7	16.7 ± 7	ICARB (April–May 2006)	Present study

reported high accumulation fraction ($A_F > 0.6$) all along the west coastal belt (over land) of India and attributed it to the anthropogenic activities over the urban centers and ports. However, excluding these pockets of high A_F , vast regions of AS were dominated by coarse mode aerosols so that on an average the A_F for the AS was only 0.42, and for 62% of the measurements, A_F was within 0.35 to 0.55. Only in 4% of the total observations, A_F was > 0.75 . This shows that, in general, super micron/coarse mode ($> 1.0 \mu\text{m}$) aerosols (probably sea salt and mineral dust) dominate the entire AS during April–May.

4.2 Effective radius

By definition, the effective radius of a poly-dispersion is the equivalent radius required for a mono-dispersion to exhibit the same total scattering properties as that of the poly-dispersion (McCartney 1976) and this is a useful parameter to characterize the scattering properties as well as changes in size distribution. Effective radius (R_{eff}) is defined as ratio of the third moment to the second moment of aerosol number size distribution and hence

$$R_{\text{eff}} = \frac{\int_{r_1}^{r_2} r^3 (dn/dr) dr}{\int_{r_1}^{r_2} r^2 (dn/dr) dr}, \quad (1)$$

where $n(r)$ is the number concentration in the size bin having a geometric mean radius r . Integration was carried out for stages 2 to 10 of the QCM, since the upper size cut-off for the first stage is

not well defined. Spatial variation of R_{eff} is shown in figure 5. Large values of R_{eff} indicate dominance of the coarse mode aerosols in the size distribution while small values indicate dominance of the accumulation mode. Variations in R_{eff} estimated from the QCM measurements were explicitly influenced by the super micron aerosol concentration and implicitly by the aerosol density (Pillai and Moorthy 2001). The overall uncertainty in the estimated number and volume size distributions and effective radius (R_{eff}) would depend on the uncertainty in the assumed value of aerosol density (ρ); percentage error in R_{eff} being as the percentage error in ρ . Over the AS, R_{eff} varied from 0.07 to 0.4 with mean value of 0.2, with 73% of the values lying between 0.13 and $0.23 \mu\text{m}$. Very high values of R_{eff} observed over the eastern and western parts of AS indicate the dominance of coarse particles in the size spectrum probably associated with the mineral dust transported from the arid regions nearby and sea salt. It should be noted that based on their measurements during the INDOEX period (February–April of 1996 to 2000), Ramachandran and Jayaraman (2002) reported considerably lower values of R_{eff} , in the range 0.095 to $0.13 \mu\text{m}$, and ascribed this to the high abundance of accumulation mode aerosols from Indian landmass. Our observations during ICARB show that over most parts of the AS (including the eastern parts), the aerosol size distribution has considerably reduced the abundance of accumulation mode particles, which contributed on an average of only 42% to the total aerosol mass loading. This shows significant temporal changes in the aerosol size distribution over the AS. This observation is also consistent with the low values (0.9 to 1.0) of

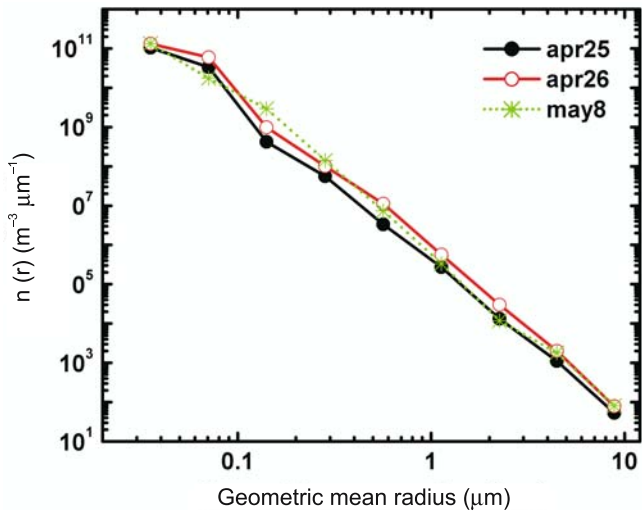


Figure 6. Number size distribution of composite aerosols for April 25, April 26 and May 8.

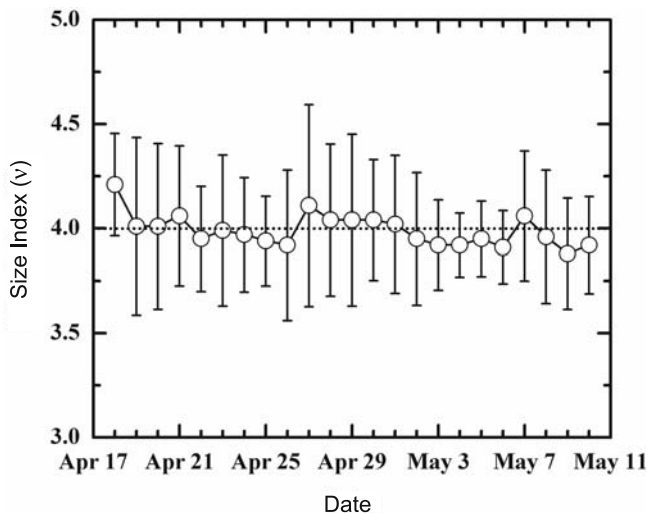


Figure 7. Daily mean variation of size index (ν) over the Arabian Sea. Vertical bars show the standard deviation and the horizontal line indicates the mean value.

Ångström exponent (α) deduced from aerosol optical depth spectra over the AS by several investigators (Satheesh and Moorthy 1997; Moorthy *et al* 2005a). The higher values of R_{eff} imply that the scattering phase function will be more pronounced in the forward direction resulting in a reduction in the radiation scattered back by the aerosols, compared to the case of low R_{eff} when accumulation fraction dominates.

4.3 Size distributions

Number size distribution (NSD) is an important requisite for the estimation of spectral extinction of solar radiation by aerosols and its impact on radiation budget of earth-atmosphere system. NSD of aerosols has been retrieved from the measured mass

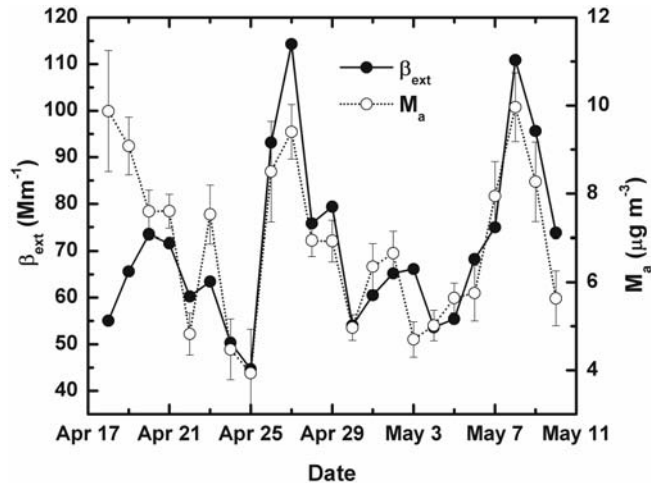


Figure 8. Comparison of the daily mean values of extinction coefficient at 550 nm with corresponding values of the accumulation mode mass concentration.

size distribution (MSD) by assuming the same density of 2 g cm^{-3} (Pillai and Moorthy 2001). Three representative mean NSDs estimated for April 25, 26, and May 8 corresponding respectively to the regions 1, 2, and 3 (as mentioned earlier) are shown in figure 6. The low resolution (in size) of the QCM does not bring out any fine features in the size spectrum of the particles; nevertheless, figure 6 shows the possibility of a fine mode below $\sim 0.05 \mu\text{m}$ and a monotonic decrease in number concentration towards larger sizes, which can be approximated by an inverse power-law distribution of the form

$$n(r) = Cr^{-\nu}, \quad (2)$$

where C is a constant and depends on the total number of particles and ν is the power law size index. The size resolution provided by the QCM being very low (limited only to four channels) in the accumulation size regime, analytical representation of the NSDs using multi-modal distributions is not possible. As such, we have approximated the distributions to the inverse power law form of equation (2) and estimated the size index ν by performing a linear regression analysis of the NSDs expressed in a log-log scale. The temporal variation of daily mean ν is given in figure 7. The errors in the regression analysis of equation (2) with the measurements to retrieve ν (arising due to the scatter of points about the regression line) are shown by the vertical bars through the points in figure 7. R^2 values were always in the range of 0.9 to 0.99 (implying a significance level of $P < 0.0001$) with no definite spatial pattern. One of the major uncertainties in the estimation of NSD and thus in ν is the shift in the radius due to the uncertainty

in the assumed density of aerosols, which can contribute nearly 20% to the estimated NSD (Pillai and Moorthy 2001). In general, ν varied from 3.8 to 4.2 with a mean value of 4 ± 0.07 and did not show any specific spatial feature. This indicates that particle heterogeneity was not highly significant. However, measurements, preferably of number concentration, with higher size resolutions are needed to examine the finer features of the NSD.

4.4 Inferring the extinction properties

Aerosol extinction coefficients (β_{ext}) have been estimated from the NSD using Mie equation

$$\beta_{\text{ext}}(\lambda) = \int \pi r^2 Q_{\text{ext}}(m, x) n(r) dr, \quad (3)$$

for a wavelength of 550 nm. In the above equation, Q_{ext} is the extinction efficiency parameter, which depends on the complex refractive index m and size parameter $x = 2\pi r/\lambda$. Complex refractive indices were taken from the INDOEX measurements made over the AS (Lubin et al 2002; Quinn et al 2002). Extinction coefficients, estimated using the the daily mean NSD in equation (3), were found to be in the range 45 to 115 Mm^{-1} ($1 \text{Mm} = 10^6 \text{m}$) with a mean value of $70.68 \pm 18 \text{Mm}^{-1}$. In figure 8, we have compared the surface extinction coefficients, thus estimated, with the mass concentration of accumulation mode aerosols (as for a given mass the accumulation mode aerosols scatter more than the coarse mode aerosols due to the large surface area). In general, the agreement is commendable and the correlation coefficient is 0.82. A comparative study revealed that extinction due to accumulation mode aerosols contributed 65 to 90% to the total extinction, even though they contributed less than 50% to the total mass. This result is also important from the stand point of radiative forcing.

5. Conclusions

A spatial characterization of the total mass concentration and size distribution of near-surface aerosols was carried out for the first time covering almost the entire Arabian Sea during ICARB. The study reveals that:

- The total mass concentrations over the Arabian Sea were remarkably low, with mean value $\sim 16.7 \pm 7 \mu\text{g m}^{-3}$ which is lower by a factor of more than 2 than the mean concentrations reported from earlier measurements over the Arabian Sea.
- Regions or pockets of high deviation from the mean pattern were observed over the central, northern and east coastal regions of the Arabian Sea.
- Accumulation mode aerosols contributed less than 50% to the total aerosol load; mean accumulation fraction being only 0.42; except in the central region of extremely low mass concentration and in the northern and coastal oceanic regions, where average A_F was > 0.50 .
- Effective radius was generally high, in the range 0.13 to 0.23 μm in about 75% of the oceanic region and had a mean value of 0.2 μm , implying reduced abundance of fine or accumulation mode particles. Higher values, going as high as 0.4 μm were observed in northern Arabian Sea and close to coastal India and Arabia.
- Number size distributions, retrieved from mass size distributions, were approximated by an inverse power law form and the size index ν was retrieved. It varied from 3.8 to 4.2 with a mean value of 4.0 ± 0.07 with no remarkable spatial features.
- The extinction coefficients at 550 nm, estimated using the retrieved number size distribution agreed very well (with a correlation coefficient of 0.82) with the variations of the accumulation mode mass concentration.

Acknowledgements

This study was supported by Geosphere Biosphere Program of the Indian Space Research Organization. Authors are greatly thankful to the Department of Ocean Development (DOD) and M Sudhakar for providing the *Sagar Kanya* and onboard facilities. We thank Nazeer Ahmed for valuable help during the cruise measurements, and the officers of *Sagar Kanya* for shipboard facilities.

References

- Ball W P, Dickerson R R, Doddridge B G, Stehr J W, Miller T L, Savoie D L and Carsey T P 2003 Bulk and size-segregated aerosol composition observed during INDOEX 1999: Overview of meteorology and continental impacts; *J. Geophys. Res.* **108** 8001, doi:10.1029/2002JD002467.
- Charlson R J, Schwartz S E, Hales J M, Cess R D, Coakley J A, Hansen J E and Hoff man D J 1992 Climate forcing by anthropogenic aerosols; *Science* **255** 423–430.
- Hess M, Koepke P and Schult I 1998 Optical properties of aerosols and clouds: The software package OPAC; *Bull. Am. Meteorol. Soc.* **79** 831–844.
- Hoell C, O'dowd C, Osborne S and Johnson D 2000 Time scale analysis of marine aerosol evolution: Lagrangian case studies under clean and polluted cloudy condition; *Tellus* **52** 423–438.

- Hoppel W A, Frick G M and Fitzgerald J W 2002 Surface source function for sea-salt and aerosol dry deposition on the ocean surface; *J. Geophys. Res.* **107** 4382, doi:10.1029/2001JD002014.
- IPCC 2007 Climate Change 2007: The Physical Science Basis. Contribution of Working Group I to the Fourth Assessment Report of the Intergovernmental Panel on Climate Change (Cambridge, United Kingdom and New York: Cambridge University Press).
- Kamra A K, Murugavel P, Pawar S D and Gopalakrishnan V 2001 Background aerosol concentration derived from the atmospheric electric conductivity measurements made over the Indian ocean during INDOEX; *J. Geophys. Res.* **106** 28,643–28,651.
- Lubin D, Satheesh S K, Macfarquar G and Heymsfield A 2002 The longwave radiative forcing of Indian Ocean tropospheric aerosol; *J. Geophys. Res.* **107** doi:10.1029/2001JD001183.
- Mc Cartney E J 1976 Optics of the Atmosphere (New York: John Wiley) 135–136.
- Moorthy K K and Saha A 2000 Aerosol study during INDOEX: Observation of enhanced aerosol activity over the mid Arabian Sea during the northern winter; *J. Atmos. Sol. Terr. Phys.* **62** 65–72.
- Moorthy K K, Saha A, Prasad B S N, Niranjana K, Jhurry D and Pillai P S 2001 Aerosol optical depth over peninsular India and adjoining oceans during INDOEX campaigns: Spatial, temporal, and spectral characteristics; *J. Geophys. Res.* **106** 28,539–28,554.
- Moorthy K K, Babu S S and Satheesh S K 2005a Aerosol characteristics and radiative impacts over the Arabian Sea during the intermonsoon season: Results from ARMEX Field Campaign; *J. Atmos. Sci.* **62** 192–206.
- Moorthy K K *et al* 2005b Wintertime spatial characteristics of boundary layer aerosols over peninsular India; *J. Geophys. Res.* **110** D08207, doi:10.1029/2004JD005520.
- Moorthy K K, Satheesh S K, Babu S S and Saha A 2005c Large latitudinal gradients and temporal heterogeneity in aerosol black carbon and its mass mixing ratio over southern and northern oceans during a transcontinental cruise experiment; *Geophys. Res. Lett.* **32** 14818, doi:10.1029/2005GL023267.
- Moorthy K K, Satheesh S K and Babu S S 2006 ICARB – An integrated Campaign for Aerosols, gases and Radiation Budget; *Proc. of SPIE*, **6408** 64080P, 0277-786X/06/\$15, doi: 10.1117/12.696110.
- Nair P R, Parameswaran K, Abraham A and Jacob S 2005 Wind-dependence of sea-salt and non-sea-salt aerosols over the oceanic environment; *J. Atmos. Solar. Terres. Phys.* **67** 884–898.
- Novakov T, Andreae M O, Gabriel R, Kirchstetter T W, Mayol-Bracero O L and Ramanathan V 2000 Origin of carbonaceous aerosols over the tropical Indian Ocean: Biomass burning or fossil fuels?; *Geophys. Res. Lett.* **27(24)** 4061–4064.
- O'Dowd C D and Smith M H 1993 Physio chemical properties of aerosols over the northeast Atlantic: Evidence for wind speed related sub micron sea-salt aerosol production; *J. Geophys. Res.* **98** 1137–1149.
- O'Dowd C D, Smith M H, Consterdine I E and Lowe J A 1997 Marine aerosol, sea-salt, and the marine sulphur cycle: A short review; *Atmos. Environ.* **31** 73–80.
- Parameswaran K, Nair P R, Rajan R and Ramana M V 1999 Aerosol loading in coastal and marine environments in the Indian Ocean region during winter season; *Curr. Sci.* **76** 947–955.
- Pillai P S and Moorthy K K 2001 Aerosol mass-size distributions at a tropical coastal environment: Response to mesoscale and synoptic scale processes; *Atmos. Environ.* **35** 4099–4122.
- Prospero J M 1979 Mineral and sea salt aerosol concentrations in various ocean regions; *J. Geophys. Res.* **84** 725–731.
- Quinn P K, Coffman D J, Bates T S, Miller T L, Johnson J E, Welton E J, Neusüss C, Miller M and Sheridan P J 2002 Aerosol optical properties during INDOEX 1999: Means, variability, and controlling factors; *J. Geophys. Res.* **107(D19)** 8020, doi:10.1029/2000JD000037.
- Ramachandran S and Jayaraman A 2002 Premonsoon aerosol loading and size distribution over the Arabian Sea and the Tropical Indian Ocean; *J. Geophys. Res.* **107** 4738, doi:10.1029/2002JD002386.
- Ramanathan V *et al* 2001 Indian Ocean Experiment: An integrated analysis of the climate and the great Indo-Asian haze; *J. Geophys. Res.* **106** 28,371–28,398.
- Sakerin S M and Kabanov D M 2002 Spatial inhomogeneities and the spectral behavior of atmospheric aerosol optical depth over the Atlantic Ocean; *J. Atmos. Sci.* **59** 484–450.
- Satheesh S K and Moorthy K K 1997 Aerosol characteristics over coastal regions of the Arabian Sea; *Tellus* **49B** 417–428.
- Satheesh S K and Srinivasan J 2002 Enhanced aerosol loading over Arabian Sea during the pre-monsoon season: Natural or anthropogenic?; *Geophys. Res. Lett.* **29** 18, doi:10.1029/2002GL015687.
- Smirnov A, Villevalde Y, O'Neill N T, Royer A and Tarussov A 1995 Aerosol optical depth over the oceans: Analysis in terms of synoptic airmass types; *J. Geophys. Res.* **100(D8)** 16,639–16,650.
- Tegen I, Lacis A A and Fung I 1996 The influence on climate forcing of mineral aerosols from disturbed soil; *Nature* **380** 419–422.
- Twomey S A 1977 The influence of pollution on the short-wave albedo of clouds; *J. Atmos. Sci.* **34** 1149–1152.
- Vinoj V and Satheesh S K 2003 Measurements of aerosol optical depth over Arabian Sea during summer monsoon season; *Geophys. Res. Lett.* **30** doi:10.1029/2002GL016664.
- Zhang L, Gong S, Padro J and Barrie L 2001 A size-segregated particle dry deposition scheme for an atmospheric aerosol module; *Atmos. Environ.* **35** 549–560.